Bol. Soc. Esp. Mat. Apl.
nº49(2009), 83–103

PREMIO SëMA JOVEN INVESTIGADOR

MODELLING AND NUMERICAL SIMULATION OF SUBMARINE SEDIMENT SHALLOW FLOWS: TRANSPORT AND AVALANCHES

ENRIQUE D. FERNÁNDEZ-NIETO

Departamento de Matemática Aplicada I, Universidad de Sevilla
E.T.S. Arquitectura. Avda, Reina Mercedes, s/n. 41012 Sevilla, Spain

edofer@us.es

Abstract

This work presents two different types of models to study submarine sediment movements and its numerical discretization by finite volume methods. First, bedload sediment transport models are introduced. They are characterized by the slow movement of the sediment layer. The movement depends on the type of interaction between the fluid and the sediment layer, that generally is very weak. Secondly, a submarine avalanches model is presented. This model takes into account the coupling between the sediment and the fluid layer. The generated tsunamis by a submarine avalanche can be studied with this model. A family of two-dimensional finite volume methods is introduced. It is based on the fact that the models are invariant under rotations. Finally, two numerical tests are considered. In the first numerical test the spread angle for a sediment bump is studied. In the second one a submarine avalanche is simulated over a bottom with a rectangular bump.

1 Introduction

This work begins by presenting some shallow models to study submarine sediment movements in channels or coastal areas.

Two different type of movements are considered. In the first part bedload sediment transport models are presented. In this case, the movement of the sediment deposited on the bottom of the channel is produced by the interaction with the fluid.

The other type of presented models study very quick movements of the sediment layer, submarine avalanches. The interaction of the movement of the sediment layer with the fluid can produce in some cases a tsunami.

After presenting these two types of models the work continues with the numerical discretization of a general two-dimensional hyperbolic system. The

Fecha de recepción: 13/12/2009. Aceptado: 14/12/2009.

property of invariance under rotation of the presented models is used in the design of the numerical scheme.

From a computational point of view, three-dimensional models are generally very expensive, so in a lot of cases it is interesting to study integrated models. In the deduction of the model, the hypothesis of shalloness of the domain is considered. The resulting model can be used by itself or combined with a three-dimensional model in areas requiring greater precision or when the considered hypothesis for the shallow model are not valid.

A first example corresponds to the well-known Saint-Venant model. It is obtained from the Navier-Stokes equations.

The steps in the deduction of Saint-Venant model, also known as Shallow Water Equations (SWE), are the following ones: First dimensionaless variables are defined depending on the charactestic horizontal and vertical lenghts of the domain. Then, a change of variable is considered, in order to write Navier-Stokes equations in terms of dimensionless variables. In this way, the system of equations can be written in terms of the aspect ratio between vertical and horizontal characteristic dimensions.

By considering that the aspect ratio is small, some terms of the system are omitted. In this way we can obtain an expression for the pressure from the vertical momentum equation. We obtain an hydrostatic pressure. It coincides with the pressure corresponding to fluid at rest. The deduction of the model finish with a process of integration over the vertical direction of the domain and a hypothesis over the vertical velocity profile.

One important hypothesis used in the deduction of shallow models is the hydrostatic pressure. This is also one of the most important restriction of aplication of the models. In some situations the pressure of the system cannot be approximated by an hydrostatic pressure. For example when there is recirculation of the fluid, that is, the vertical acceleration of the fluid is am important effect.

A typical example is to simulate the evolution of a dam break. For this example it is well known that at the beginning of the movement the velocity of the fluid predicted by using SWE is bigger than the velocity obtained with Navier-Stokes equations (see [27]). This is a consequence of the hydrostatic pressure. Nevertheless, the results obtained with SWE and Navier-Stokes equations for the evolution of the water depth far from the dam are close. So, the SWE approach is appropriate for large computational domains or large time simulations, due to a smaller computational cost.

An example of long time simulations is the study of summerged sediment evolution. In this problem we consider that the bottom of the domain is composed of a fixed component and a mobile sediment layer (See [24], [11], [14]). The evolution of the sediment layer is very slow, because its evolution is produced by the interaction with the fluid. The interaction between the fluid and the sediment layer depends on the friction between these two layers. It is introduced in the problem via the definition of the solid transport discharge (see [15], [21]), defining a continuity equation. So, we have a coupled system

defined by the SWE and the continuity equation for the sediment evolution.

Another type of sediment evolution can be observed when there is a sedimentation over the bottom and the sediment layer colapses, by producing a submarine avalanche. In [9] it is proposed a two layers SWE system where the submarine avalanche and the eventual generated tsunami can be studied. The first layer corresponds to the fluid and the second one to the sediment layer.

For the sediment layer a Savage-Hutter type model is considered. The pionering work of Savage-Hutter [28] derives a model to describe granular flows over a slopping plane based on Mohr-Coulomb considerations: a Coulomb friction is assumed to reflect the avalanche/bottom interaction and the normal stress tensor is defined by a constitutive law relating the longitudinal and the normal stresses through a proportionality factor.

One of the characteristics of the model proposed in [9] is that the definition of the Coulomb friction term takes into account bouyancy effects, because we are studying submarine avalanches. Another characteristic is that, depending on the aspect ratio between the water density and the sediment density, the movement of the sediment avalanches can be more or less influenced by the presence of the fluid. The submarine avalanches produces a movement on the fluid layer, whose consequence can be a tsunami.

There are many other effects that can be studied around summerged sediments, such as suspension, erosion or deposition effects (see [18] for more details).

In this work we focus on the presentation of the models corresponding to sediment bedload transport and submarine avalanches. These models can be written under the general formulation

$$\frac{\partial U}{\partial t} + \frac{\partial F_1}{\partial x_1}(U) + \frac{\partial F_2}{\partial x_2}(U) = B_1(U)\frac{\partial W}{\partial x_1} + B_2(U)\frac{\partial U}{\partial x_2} + S_1(U)\frac{\partial H}{\partial x_1} + S_2(U)\frac{\partial H}{\partial x_2}. \tag{1}$$

where the unknown $U(\mathbf{x}, t)$ is defined in the domain $D \times (0, T)$, where D is a subset of $\mathbb{R}^2$, with values in an open subset Ω of $\mathbb{R}^N$; F_i, $i = 1, 2$ are regular functions from Ω to $\mathbb{R}^N$; B_i, $i = 1, 2$ are regular function matrices from Ω to $\mathcal{M}_{N\times N}(\mathbb{R})$; S_i, $i = 1, 2$ are defined from D to $\mathbb{R}^N$; and $H(\mathbf{x})$ is a known function from D to $\mathbb{R}$.

This general framework includes particular cases corresponding to conservation laws ($B_i = 0$, $S_i = 0$, $i = 1, 2$); hyperbolic systems with source terms, or balance laws ($B_i = 0$, $i = 1, 2$); and nonconservative system, corresponding to coupled hyperbolic systems.

This work is organized as follows: In Section 2 we focus on bedload sediment transport models. Theoretical and experimental models are presented by including a brief description of the principles considered to define the solid transport discharge. In Section 3 we present a simplied 2D extention of the model proposed in [9] for submarine avalanches. Section 4 is devoted to the presentation of a family of finite volume methods. Finally, in Section 5 we present two numerical tests. In the first numerical test the spread angle for a

sediment bump is studied. In the second one a submarine avalanche is simulated over a bottom with a rectangular bump.

2 Bedload sediment transport

In this work we consider two different types of submarine sediment movements. In this section we study the transport of sediment over the bottom by interaction with the fluid.

Sediment transports are classified into three types: bedload, saltation and suspension. Bedload transport is defined as the type of transport where sediment grains roll or slide along the bed. Saltation is produced when single grains jump over the bed, losing for instants the contact with the soil. Sediment is suspended when the flux is intense enough such as the sediment grains reach height over the bed.

We only consider the case of bedload sediment transport. To study this problem a coupled system defined by the Shallow Water equations and a continuity equation can be considered. The continuity equation depends on the definition of the solid transport discharge.

The definition of the solid transport discharge is done by empirical laws. Some of them are deterministic formulae and other are based on probabilistic terms. Some of the proposed models have been proposed by the following authors: Grass [13], Meyer-Peter&Müller's [17], Van Rijn's [30], Nielsen [21], Kalinske [16], Einstein [8], etc.

In the following subsection we present the formulation for a family of deterministic beload sediment transport models.

We denote by z_s the height of the sediment layer and z_b the fixed bottom. By h we denote the height of the water layer. The discharge vector is denoted by $\vec{q} = (q_1, q_2) = h\vec{u}$, where by $\vec{u} = (u_1, u_2)$ we denote the vector of velocities at x and y directions. Then, the model can be written as follows,

$$\begin{cases} \partial_t h + \partial_x(q_1) + \partial_y(q_2) = 0, \\ \partial_t(q_1) + \partial_x(\dfrac{q_1^2}{h} + \dfrac{1}{2}gh^2) + \partial_y(\dfrac{q_1 q_2}{h}) = -gh\partial_x(z_s + z_b) - ghS_{f\,1}, \\ \partial_t(q_2) + \partial_x(\dfrac{q_1 q_2}{h}) + \partial_y(\dfrac{q_2^2}{h} + \dfrac{1}{2}gh^2) = -gh\partial_y(z_s + z_b) - ghS_{f\,2}, \\ \partial_t z_s + \xi\partial_x(\mathcal{Q}_{s\,x}(h, \vec{q})) + \xi\partial_y(\mathcal{Q}_{s\,y}(h, \vec{q})) = 0. \end{cases}$$

where g is the gravity constant, $\xi = 1/(1 - \psi_0)$ being ψ_0 the porosity of the sediment layer and $\mathcal{Q}_s = (\mathcal{Q}_{s\,x}, \mathcal{Q}_{s\,y})$ the solid transport discharge vector formula. For friction term $\vec{S}_f = (S_{f\,1}, S_{f\,2})$ we consider Manning laws,

$$\vec{S}_f = \frac{n^2\|\vec{u}\|}{R_h^{4/3}}\vec{u},$$

where n is the bed roughness coefficient and R_h is the hydraulic ratio.

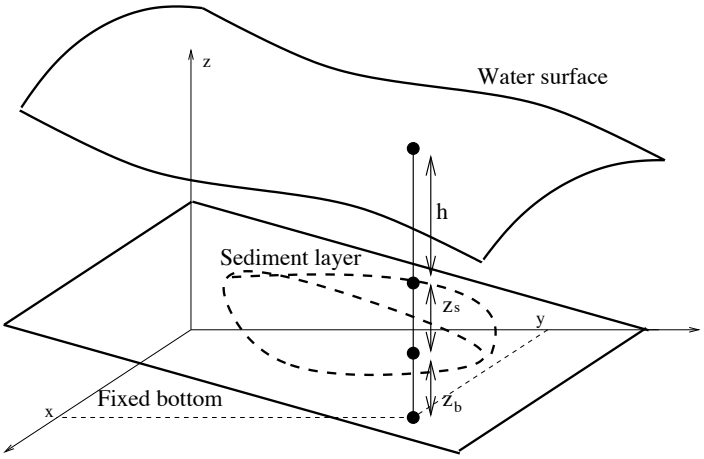

Figure 1: Notation: Bedload sediment transport

2.1 Solid transport discharge formulae

The continuity equation describing the evolution of the sediment layer is defined in terms of the solid transport discharge $\mathcal{Q}_s = (\mathcal{Q}_{s\,x}, \mathcal{Q}_{s\,y})$.

If by q_s we denote the solid transport discharge for a one-dimensional model, then,

$$\mathcal{Q}_{s,x}(h,\vec{q}) = \frac{q_1}{\|\vec{q}\|}\left|q_s(h,\|\vec{q}\|)\right|, \quad \mathcal{Q}_{s,y}(h,\vec{q}) = \frac{q_2}{\|\vec{q}\|}\left|q_s(h,\|\vec{q}\|)\right|, \tag{2}$$

where $\|\vec{q}\| = \sqrt{q_1^2 + q_2^2}$.

As we mentioned previously, there is a lot of formulae, which are deduced empirically and corresponds to different ranges of applycation (see [24]).

One of the simpler models was proposed by Grass (see [13]). This model supposes that the solid transport discharge is proportional to a power of the velocity,

$$q_b = Au|u|^k,$$

where A and k are two parameters of the model. Constant A depends on the interaction between the fluid and the sediment. Generally it is a small value, $A = \mathcal{O}(10^{-3})$ (See [2]). A typical value of k is $k = 2$.

This is a theoretical model, whose main characteristic is that the sediment layer moves when the fluid layer does. For other type of models, which are deduced in terms of empirical data, the sediment layer does not move for any movement of the fluid. The sediment moves when the shear stress, τ, is bigger than a critical shear stress, τ_c.

The definition of the shear stress depends on the definition of the friction term $\vec{S}_f$,

$$\tau = \gamma R_h \|S_f\|.$$

where γ denotes the specific weight of the fluid, $\gamma = g\rho$, where ρ is the water density.

Usually, the model is presented in dimensionless form. Then, the definition of the solid transport discharge is done in terms of the difference between the dimensionless shear stress, τ^* and a dimensionless critical shear stress, τ_c^*.

The dimensionless solid transport discharge, q_b^*, is written in terms of the mean grain size, d_i, and the characteristic settling velocity $\sqrt{(G-1)gd_i}$,

$$q_b^* = \frac{q_b}{d_i\sqrt{(G-1)gd_i}},$$

where $G = \rho_s/\rho$ is the relative density, being ρ_s the sediment density. The dimensionless shear stress τ^* (see [15]) is defined in terms of the ratio between drag forces, $F_D = \tau d_i^2$, and the summerged weight, $F_S = (\gamma_s - \gamma)d_i^3$, where $\gamma_s = g\rho_s$ is the specific sediment weight. We have,

$$\tau^* = \frac{\tau}{(\gamma_s - \gamma)d_i} = \frac{R_h\|S_f\|}{(G-1)d_i}.$$

Analogously the critical shear stress is defined as

$$\tau_c^* = \frac{\tau_c^*}{(\gamma_s - \gamma)d_i}.$$

A great number of proposed models can be written under the following formulation,

$$q_b^* = f(h, q, \tau)(K\,\tau^* - \tau_c^*)_+^m.$$

where power m, constant K and function f depend on the model. This formulation includes that the movement of the sediment layer begins only when the shear stress is bigger than the critical shear stress, because it depends on the positive part of the difference between τ^* and τ_c^*. Constant K is usually set to 1, although it can be defined as the ratio between the the bed roughness coefficient of the sediment layer and the fixed bottom.

Some models corresponds to:

- Meyer-Peter&Müller: $q_b^* = 8(\tau^* - \tau_c^*)_+^{3/2}$
- Fernández Luque & Van Beek: $q_b^* = 5.7(\tau^* - \tau_c^*)_+^{1/3}$
- Nielsen: $q_b^* = 12\sqrt{\tau^*}(\tau^* - \tau_c^*)_+$

All these formulae have a range of application in function of grain size, the slope of the bottom, the Froude number and the relative density G. For example in the case of the Meyer-Peter&Müller model it is applied for a $0.4 \leq d_i \leq 29$ $mm.$, slopes of the bottom smaller than 0.02 and $1.25 \leq G \leq 4.2$ (see [24] and [11] for more details).

To determine τ_c^* many experiments have been performed in different works. Concretely, Shields proposed the well-known Shields-diagram.

In [31] two grass type models are proposed, in the sense that they do not depend on a critical shear stress. We denote the models presented in [31] by $\mathcal{MS}1$ and $\mathcal{MS}2$, defined by:

- $\mathcal{MS}1$: $q_b = Ahu|u|^k$ with $0 < k < 1/2$,
- $\mathcal{MS}2$: $q_b = Ah(1 + log(1 + |u|^2))u$,

where A is the constant of interaction between the fluid and the sediment.

3 Submarine avalanches model

Submarine avalanches or landslides are poorly studied compared to aerial avalanches. This is however a key issue in geophysics. For example, submarine granular flows driven by gravity participate in the evolution of the sea floor and in particular of the continental margins.

In [9] a two-layer 1D model is presented to study submarine avalanches. The sediment layer is modelled as a Savage-Hutter type system (see [28]). It is summerged in a fluid, that is considered as the other layer of the model.

Savage-Hutter model is characterized by the presence of a Coulomb friction term. This term opposes to the movement of the avalanches, and its definition depends on a critical value in terms of the pressure at the bottom and a friction angle. The definition of the Coulomb friction term for the model proposed in [9] also includes the bouyancy effect.

In this section we present a 2D simplified extention of the model proposed in [9]. With subindex 1 we denote the unknowns corresponding to the fluid layer: h_1 is the height of the fluid layer and $\vec{q}_1 = (q_{11}, q_{12})$ is the vector of discharges. Index 2 corresponds to the sediment layer: by h_2 we denote denote the height of the sediment layer and $\vec{q}_2 = (q_{21}, q_{22})$ is the discharge. The fixed bottom topography is described by function z_b (See Figure 2).

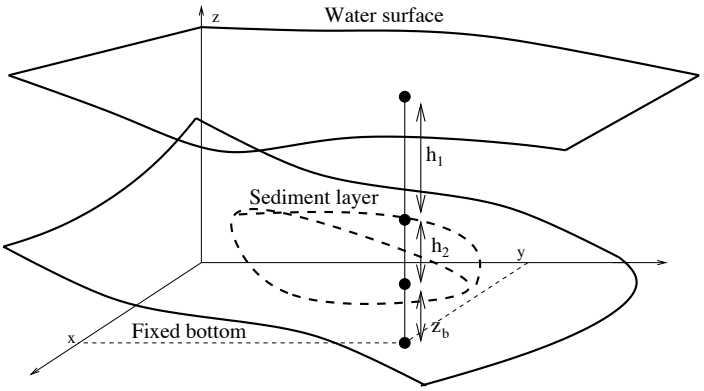

Figure 2: Notation, 2D submarine avalanches

By simplicity we consider a fixed bottom with small slope. Then, we obtain the following model:

$$\left\{\begin{array}{l}
\partial_t h_1 + \partial_x(q_{11}) + \partial_y(q_{12}) = 0,\\
\partial_t(q_{11}) + \partial_x(\frac{q_{11}^2}{h_1} + g\frac{h_1^2}{2}) + \partial_y(\frac{q_{11}q_{12}}{h_1}) = -g\,h_1\partial_x(z_b + h_2),\\
\partial_t(q_{12}) + \partial_x(\frac{q_{11}q_{12}}{h_1}) + \partial_y(\frac{q_{12}^2}{h_1} + g\,\frac{h_1^2}{2}) = -g\,h_1\,\partial_y(z_b + h_2),\\
\partial_t h_2 + \partial_x(q_{21}) + \partial_y(q_{22}) = 0,\\
\partial_t(q_{21}) + \partial_x(\frac{q_{21}^2}{h_2} + g\frac{h_2^2}{2}) + \partial_y(\frac{q_{21}q_{22}}{h_2}) = -gh_2\partial_x(z_b + rh_1) + \mathcal{T}_x,\\
\partial_t(q_{22}) + \partial_x(\frac{q_{21}q_{22}}{h_2}) + \partial_y(\frac{q_{22}^2}{h_2} + g\frac{h_2^2}{2}) = -gh_2\partial_y(z_b + rh_1) + \mathcal{T}_y.
\end{array}\right.$$

where $r = \rho_1/\rho_2$ and $\mathcal{T} = (\mathcal{T}_x, \mathcal{T}_y)$ denotes the Coulomb friction term,

$$\begin{array}{ll}
\text{If } |\mathcal{T}| \geq \sigma_c & \Rightarrow \quad \mathcal{T} = -g(1-r)h_2\dfrac{\vec{u}_2}{|\vec{u}_2|}\mu.\\
\text{If } |\mathcal{T}| < \sigma_c & \Rightarrow \quad \vec{u}_2 = 0.
\end{array} \tag{3}$$

with $\sigma_c = g(1-r)h_2\tan(\delta_0)$. The definition of the frictional term μ depends on the model. The simplest definition corresponds to

$$\mu = \tan(\delta_0), \tag{4}$$

where δ_0 is the frictional angle. Altough some other definitions have been proposed in the bibliography (see [19], [25]). For example, in order to incorporate turbulence effects McDougall and Hungr [20] proposed to add to the definition of $\mathcal{T}$ a turbulent term proportional to $|\vec{u}_2|^2$. Other definition, deduced from experimental data, has been proposed by Pouliquen (see [26]). It depends on the Froude number, the thickness of the sediment layer, the mean diameter of the sediment, the velocity of the moving layer, and two friction angles.

4 Numerical scheme

The models that we have presented previously can be written under the following structure,

$$\partial_t W + \partial_{x_1} F_1(W) + \partial_{x_2} F_2(W) = B_1(W)\partial_{x_1} W + B_2(W)\partial_{x_2} W. \tag{5}$$

These models verify the property of invariance under rotations. If $\eta = (\eta_1, \eta_2)$ is a unitary vector, we define

$$T_\eta = \begin{pmatrix} 1 & 0 & 0 & 0\\ 0 & \eta_1 & \eta_2 & 0\\ 0 & -\eta_2 & \eta_1 & 0\\ 0 & 0 & 0 & 1 \end{pmatrix}, \quad \text{or} \quad T_\eta = \begin{pmatrix} 1 & 0 & 0 & 0 & 0 & 0\\ 0 & \eta_1 & \eta_2 & 0 & 0 & 0\\ 0 & -\eta_2 & \eta_1 & 0 & 0 & 0\\ 0 & 0 & 0 & 1 & 0 & 0\\ 0 & 0 & 0 & 0 & \eta_1 & \eta_2\\ 0 & 0 & 0 & 0 & -\eta_2 & \eta_1 \end{pmatrix},$$

for the sediment transport model and the submarine avalanches model, respectively.

We denote $F_\eta = F_1\eta_1 + F_2\eta_2$ and $\mathcal{B}(W) = (B_1(W), B_2(W))$. Then, by the invariance under rotations property we have,

$$F_\eta = T_\eta^{-1} F_1(T_\eta W). \tag{6}$$

and

$$T_\eta(\mathcal{B}(W)\cdot\eta) = B_1(T_\eta W). \tag{7}$$

For example, for the sediment transport model, we can see that (6) is verified by using the definition of the solid transport discharge (2) and the proof of invariance under rotations for Shallow Water Equations (See for example [29]).

Moreover, it is easy to see that, for a given unitary vector η, system (5) can be rewritten as follows,

$$\partial_t(W) + \partial_\eta F_\eta + \partial_{\eta^\perp} F_{\eta^\perp} = (\mathcal{B}(W)\cdot\eta)\partial_\eta W + (\mathcal{B}(W)\cdot\eta^\perp)\partial_{\eta^\perp} W.$$

By multiplying previous system by T_η and by using (6), (7) we obtain

$$\partial_t(T_\eta W) + F_1(T_\eta W) = B_1(T_\eta W)\partial_\eta W + \mathcal{P}_{\eta^\perp}, \tag{8}$$

where

$$\mathcal{P}_{\eta^\perp} = T_\eta\Big(- \partial_{\eta^\perp} F_{\eta^\perp}(W) + (\mathcal{B}(W)\cdot\eta^\perp)\partial_{\eta^\perp} W\Big).$$

The design of the numerical scheme is done by using (8) at each edge of a mesh, being η the normal vector to the edge (see [1], [3] and [10]).

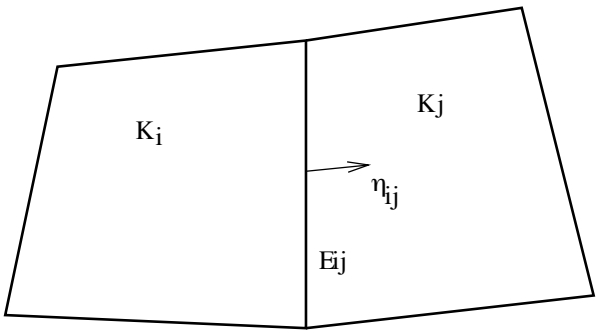

Figure 3: Notation, control volumes

We begin by considering a mesh of the domain Ω into control volumes. We denote the volumes that define the mesh by K_i. By $E_{i\,j}$ we denote the common edge between the volumes K_i and K_j. And $\eta_{i\,j}$ is the unitary normal vector to $E_{i\,j}$ outward to K_i (See Figure 3). The structure of the 2D finite volume method is:

$$W_i^{n+1} = W_i^n - \frac{\Delta t}{|K_i|}\sum_{j\in K_i}|E_{i\,j}|\Phi(W_i^n, W_j^n, \eta_{i\,j}) + \frac{\Delta t}{2|K_i|}\sum_{j\in K_i}|E_{i\,j}|\mathcal{B}_{\eta_{ij}}(W_j^n - W_i^n). \tag{9}$$

where $\Phi(W_i^n, W_j^n, \eta_{i\,j})$ is an approximation of the normal flux associated to the edge $E_{i\,j}$. And $\mathcal{B}_{\eta_{ij}}$ is an approximation of $\mathcal{B}(W)\cdot\eta_{i\,j}$.

By using (7) we can define

$$\mathcal{B}_{\eta_{ij}} = T_{\eta_{ij}}^{-1} B_1(T_{\eta_{ij}} W_{(i+j)/2}).$$

And, by using (6), we define

$$\Phi(W_i, W_j, \eta_{ij}) = T_{\eta_{ij}}^{-1}\phi(T_{\eta_{i\,j}} W_i, T_{\eta_{i\,j}} W_j),$$

where $\phi(W_i, W_j)$ is the numerical flux function of a 1D system, obtained from the 2D system by a projection over $\eta_{i\,j}$. The 1D system is defined by (8) with $\eta = \eta_{i\,j}$, after to neglect the term $\mathcal{P}_{\eta_{i\,j}^{\perp}}$. We have the system,

$$\partial_t(T_{\eta_{ij}} W) + \partial_{\eta_{i\,j}} F_1(T_{\eta_{ij}} W) = B_1(T_{\eta_{ij}} W)\partial_{\eta_{ij}} W. \tag{10}$$

For the sediment transport model and the submarine avalanche model, presented previously, we have

$$T_\eta W = \begin{pmatrix} h_1 \\ q_{1,\eta} \\ q_{1,\eta^\perp} \\ z_b \end{pmatrix}, \quad \text{and} \quad T_\eta W = \begin{pmatrix} h_1 \\ q_{1,\eta} \\ q_{1,\eta^\perp} \\ h_2 \\ q_{2,\eta} \\ q_{2,\eta^\perp} \end{pmatrix},$$

respectively. Then, for the sediment transport model, system (10) reduces to the following one:

$$\begin{cases} \partial_t h_1 + \partial_\eta(q_{1,\eta}) = 0, \\ \partial_t(q_{1,\eta}) + \partial_\eta(\dfrac{q_{1,\eta}^2}{h_0} + g\dfrac{h_1^2}{2}) = -g h_1 \partial_\eta(z_b - H), \\ \partial_t(q_{1,\eta^\perp}) + \partial_\eta(\dfrac{q_{1,\eta} q_{1,\eta^\perp}}{h_0}) = 0, \\ \partial_t(z_b) + \partial_\eta(q_b(h, \|(q_{1,\eta}, q_{1,\eta^\perp})\|)) = 0. \end{cases} \tag{11}$$

For the submarine avalanches model, system (10) corresponds to:

$$\begin{cases} \partial_t h_1 + \partial_\eta(q_{1,\eta}) = 0, \\ \partial_t(q_{1,\eta}) + \partial_\eta(\dfrac{q_{1,\eta}^2}{h_1} + g\dfrac{h_1^2}{2}) = -gh_1\partial_\eta z_b - gh_1\partial_\eta h_2, \\ \partial_t(q_{1,\eta^\perp}) + \partial_\eta(\dfrac{q_{1,\eta}q_{1,\eta^\perp}}{h_1}) = 0, \\ \partial_t h_2 + \partial_\eta(q_{2,\eta}) = 0, \\ \partial_t(q_{2,\eta}) + \partial_\eta(\dfrac{q_{2,\eta}^2}{h_2} + g\dfrac{h_2^2}{2}) = -gh_2\partial_\eta z_b - rgch_2\partial_\eta h_1, \\ \partial_t(q_{2,\eta^\perp}) + \partial_\eta(\dfrac{q_{2,\eta}q_{2,\eta^\perp}}{h_1}) = 0. \end{cases} \tag{12}$$

System (11) has a linearly degenerated field. And system (12) has two linearly degenerated fields. Moreover, they are associated to a passive escalar. That is, the evolution of the unknown corresponding to the passive escalar does not have influence over the other unknowns of the problem. For (11), the passive scalar is $q_{\eta^\perp}$. For (12), there are two passive scalars, corresponding to the unkowns $q_{1,\eta^\perp}$ and $q_{2,\eta^\perp}$.

Previously to define the numerical scheme we remark another property. The components of the flux functions corresponding to the equations for the passive scalars are related to the components of the flux corresponding to the mass conservation equations (see equations (11) and (12)).

For the mass conservation law the component of the flux function is $q_{l,\eta}$, $l = 1, 2$ (we denote $q_{1,\eta} = q_\eta$ for the sediment transport model). And the component of the flux functions corresponding to passive scalar evolution $q_{l,\eta^\perp}$ is $\left(q_{l,\eta}\dfrac{q_{l,\eta^\perp}}{h_l}\right)$, $l = 1, 2$.

That is, the flux corresponding to the passive scalar is the product of the component of the flux function for the mass conservation equation and the concentration of the passive scalar: $(q_{l,\eta^\perp}/h_l)$, $l = 1, 2$.

Then, we can generalize the technique introduced in the definition of the HLLC method for the Shallow Water equations, by using a similar relationship. To define the numerical flux function, the component for the passive scalar is defined in terms of the numerical flux function for the mass conservation component and the concentration of the passive scalar.

In this way, the definition of $\phi(T_{\eta_{i\,j}}W_i, T_{\eta_{i\,j}}W_j)$ is done by components. In a first step we define the components of the numerical flux function corresponding to non passive scalar unkowns. In a second step we define the components of the numerical flux function associated to the passive scalars.

To define the numerical scheme we introduce the following notation. By $\mathcal{N}$ we denote the set of index associated to the non passive scalar unknowns. We

have $\mathcal{N} = \{1, 2, 4\}$ for the sediment transport model and $\mathcal{N} = \{1, 2, 4, 5\}$, for the submarine avalanches model. We also denote by $[\phi]_{\mathcal{N}}$ the vector defined by the components of ϕ with index in $\mathcal{N}$.

The definition of the numerical scheme is done in the following two steps.

• **Step 1:** Definition of $[\phi]_{\mathcal{N}}$.

We consider a family of finite volume methods, that can be written under the following notation (See [4]):

$$[\varphi(V_i, V_j)]_{\mathcal{N}} = \frac{[F_1(V_j)]_{\mathcal{N}} + [F_1(V_i)]_{\mathcal{N}}}{2} - \mathcal{D}(V_i, V_j)([V_j - V_i]_{\mathcal{N}}).$$

By $\mathcal{D}$ we denote the numerical viscosity matrix of the numerical scheme (see [12]). For different definitions of the matrix $\mathcal{D}$ we obtain different methods such as Roe, Lax-Wendroff, Rusanov or Lax-Friedrichs. For example, Roe method corresponds to define

$$\mathcal{D}(V_i, V_j) = |\mathcal{A}_{ij}|,$$

the absolute value of Roe matrix. By $\mathcal{A}_{ij}$ we denote the Roe matrix associated to system (10) for the equations of the set $\mathcal{N}$.

As in system (10) a nonconservative term appears, the definition of Roe matrix depends on the choice of a family of paths (See [22], [5], [23]).

For a given family of paths, $\varphi(s, [V_i]_{\mathcal{N}}, [V_j]_{\mathcal{N}})$ with $s \in [0, 1]$, verifying

$$\varphi(0, [V_i]_{\mathcal{N}}, [V_j]_{\mathcal{N}}) = [V_i]_{\mathcal{N}}, \quad \varphi(1, [V_i]_{\mathcal{N}}, [V_j]_{\mathcal{N}}) = [V_j]_{\mathcal{N}},$$

Roe matrix is defined as follows (see [22] for details),

$$\mathcal{A}_{i\,j}([V_j - V_i]_{\mathcal{N}}) = [F_1(V_j) - F_1(V_i)]_{\mathcal{N}} - \int_0^1 B_1(\varphi(s, [V_i]_{\mathcal{N}}, [V_j]_{\mathcal{N}}))\partial_s \varphi(s, [V_i]_{\mathcal{N}}, [V_j]_{\mathcal{N}}) ds.$$

We suppose that the Roe matrix $\mathcal{A}_{ij}$ can be diagonalized, $\mathcal{A}_{i\,j} = \mathcal{K}_{ij}\mathcal{L}_{ij}\mathcal{K}_{ij}^{-1}$, where $\mathcal{K}_{ij}$ is the matrix defined by their eigenvectors and $\mathcal{L}_{ij}$ is the diagonal matrix defined by the eigenvalues,

$$\mathcal{L}_{ij} = \text{diag}(\lambda_{ij,l}, l = 1, ., N),$$

with $N = 3$ for the sediment transport model and $N = 4$ for the submarine avalanche one. Then, the absolute value of Roe matrix is defined as follows,

$$|\mathcal{A}_{ij}| = \mathcal{K}_{ij}|\mathcal{L}_{ij}|\mathcal{K}_{ij}^{-1}, \text{ with } |\mathcal{L}_{ij}| = \text{diag}(|\lambda_{ij,l}|, l = 1, ., N).$$

• **Step 2:** In this second step we define the components of the numerical flux functions corresponding to the equations of the passive escalar. For the sediment transport model we define $[\phi]_3$ and for the submarine avalanches model we define $[\phi]_3$ and $[\phi_6]$. The third components are defined un terms of the first components of the numerical flux functions, and the sixth component in terms of the fourth component of the numerical flux functions.

By following the idea of HLLC method we propose the following definitions:

$$[\phi]_3 = \Big([\phi]_1\Big)\mathcal{C}^*_{1,\eta^\perp_{ij}}, \quad [\phi]_6 = \Big([\phi]_3\Big)\mathcal{C}^*_{2,\eta^\perp_{ij}}.$$

By $\mathcal{C}^*_{l,\eta^\perp_{ij}}$, $l = 1, 2$ we denote an uncentered approximation of the concentration of pasive scalar, $(q_{l,\eta^\perp_{ij}}/h_l)$, $l = 1, 2$, over the edge E_{ij}. The definition is the following one:

$$\mathcal{C}^*_{l,\eta^\perp_{ij}} = \begin{cases} q_{l\,i,\eta_{ij}}/h_l & \text{if } S^*_{l,ij} < 0, \\ q_{l\,j,\eta_{ij}}/h_l & \text{if } S^*_{l,ij} > 0, \end{cases} \qquad l = 1, 2 \tag{13}$$

The value $S^*_{l,ij}$, $l = 1, 2$ is an approximation of the velocity $(q_{l,\eta_{ij}}/h_l)$, $l = 1, 2$ over the edge E_{ij}. We can use for example $S^*_{l,ij} = u_{l,ij}$, the averaged Roe velocity. Some other definitions are possible, as the one proposed in [10].

5 Numerical tests

5.1 Test 1: Bedload sediment transport: expansion angle

The objective of this test is to compare classical Grass model with the models proposed in [31], described in Section 2. We have denoted these two models by $\mathcal{M}S1$ and $\mathcal{M}S2$.

In order to understand the properties and differences between Grass, $\mathcal{M}S1$ and $\mathcal{M}S2$ models, we consider the test that we describe in what follows.

When the interaction between the fluid and the sediment is weak, the spread angle of a sediment bump can be estimated analytically. DeVriend in [6, 7] deduces the following formula for the spread angle, α:

$$\tan\alpha = \frac{3\,T_u\,\sqrt{3}}{9\,T_u - 8\,T_h}. \tag{14}$$

where T_u and T_h is defined in function of the solid transport discharge expresed as a function of the height of the fluid and the velocity modul: $q_s = q_s(h, |u|)$. Concretely,

$$T_u = \frac{u}{S_b(h,u)}\,\frac{\partial q_s(h,|u|)}{\partial |u|} \;-\; 1, \quad T_h = \frac{h}{q_s(h,|u|)}\,\frac{\partial q_s(h,|u|)}{\partial h} - 1.$$

For $\mathcal{M}S1$ model we obtain,

$$q_s(h,|u|) = A\,h\,|u|^{k+1}.$$

Then, by applying (14) we have,

$$\tan\alpha = \frac{\sqrt{3}}{3}$$

That is, the spread angle is independent of the parameter k. We obtaint that the spread angle is $\alpha = 30^o$, for any value of k.

For $\mathcal{M}S2$ model we have

$$q_s(h,|u|) = A\,h|u|(1+log(1+|u|^2)).$$

We also obtain that $\alpha = 30^o$ for any value of k. Nevertheles, for Grass model, defined by

$$q_s(h,|u|) = A_g\,|u|^{k+1}.$$

we obtain that

$$\tan\alpha = \frac{3\,k\sqrt{3}}{9\,k\,\sqrt{3}+8}.$$

That is, the spread angle depends on the value of parameter k. Moreover, we obtain that the limit of the angle is 30^o. A typical value for parameter k is $k=2$. For this value we obtain $\alpha = 21.78^o$.

To study the spread angle we simulate numerically the evolution of a sediment bump for these three models. The constant of interaction is set to $A = 0.01$. The domain is $[0,L]\times[0,L]$ with $L = 1000$. The mesh of the domain is composed by 7600 edge type control volumes. As boundary condition we impose $q_y = 0$ for $y = 0$ and $y = L$. At $x = 0$ we impose the discharge $\vec{q} = (10,0)$. And at $x = L$ we impose free boundary conditions. And as initial conditions,

$$h(x,y,0) = 10.1 - z_b(x,y,0), \quad q_x(x,y,0) = 10, \quad q_y(x,y,0) = 0;$$

with

$$z_b(x,y,0) = \begin{cases} 0.1 + \sin^2\left(\frac{\pi(x-300)}{200}\right)\sin^2\left(\frac{\pi(y-400)}{200}\right) & \text{if } \begin{array}{l} 300 \le x \le 500, \\ 400 \le y \le 600, \end{array} \\ 0.1 & \text{otherwise.} \end{cases}$$

In Figure 4 we present the evolution of the sediment bump. We superpose the level curves corresponding to the initial condition, an intermediate time, and the final time of simulation. The final time simulation is $t = 36000$ s. for $\mathcal{M}S1$ and Grass model. Nevertheless, for $\mathcal{M}S2$ model the final time is $t = 14000$ s. In these figures we also represent the lines corresponding to $\alpha = 21.78^o$ and $\alpha = 30^o$.

In Figure 4(a) we observe that, as predicted by the approximation of DeVriend's formula, the numerical results obtained with Grass model follows an spread angle close to $\alpha = 21.78^o$. And in Figure 4(b) we observe that the spread angle for model $\mathcal{M}S1$ is closer to $\alpha = 30^o$.

In Figure 4(c) we compare the level curves for the final time for Grass and $\mathcal{M}S1$ models. We can observe that altough the spread angle for these models are different, the evolution for the position of the bump is nearly analogous. Nevertheless, as we can see in Figure 4(d), when we compare it to model $\mathcal{M}S2$, with spread angle $\alpha = 30^o$, the evolution time of the bump is very different.

The difference in the evolution of the sediment bump for Grass or $\mathcal{M}S1$ model in comparison with $\mathcal{M}S2$ is the logaritmic formulation. Usually, the

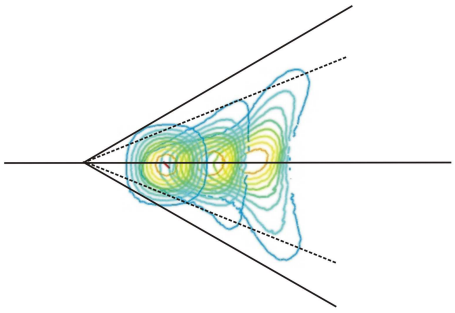

(a) Grass model, $t = 36000$ s.

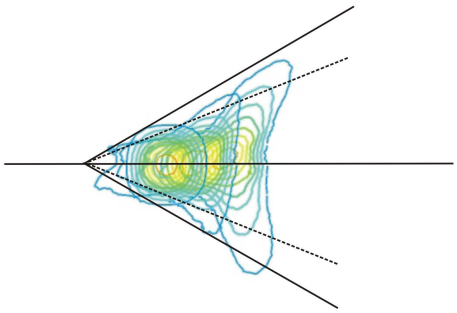

(b) $\mathcal{M}S1$ model, $t = 36000$ s.

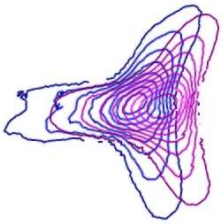

(c) $t = 36000$ s. $\mathcal{M}S1$ model (black lines) and Grass model (magenta lines).

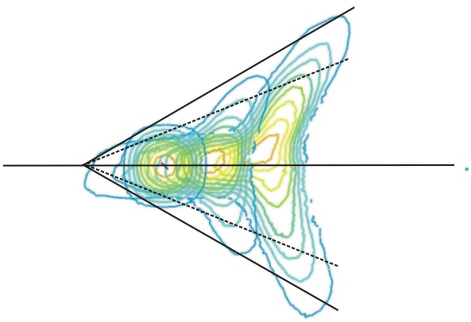

(d) $\mathcal{M}S2$ model, $t = 14000$ s.

Figure 4: Spread angles. Level curves of the sediment bump evolution

laboratory experiments are done with small velocities of the fluid. Following these results, the proposed models are written in terms of a power of the velocity. When we use the model for higger velocities, as we are using a power of the velocity, the values of the solid transport discharge are very high. Nevertheless, the formulation in form of logaritmic allows to control the range of the solid transport discharge with high velocities.

5.2 Test 2: submarine avalanche

In this test we present an application of the submarine avalanche model. We consider that the fixed bottom is flat except by a bump in form of rectangle. And we define the sediment layer as a cilinder next to the bump. We study the influence of the bump, by comparing the amplitude and velocity of the front in the water surface.

The domain is $[0,1]\times[0,1]$ that is discretized by a regular mesh of 150×150 volumes. The CFL condition is 0.8. We impose free boundary conditions over all the edges of the domain. The fixed bottom function is

$$z_b(x,y)=\begin{cases} 0.025 & \text{if } x\in[0.6,0.7],\\ 0 & \text{otherwise.}\end{cases}$$

As initial conditions we impose fluid and sediment at rest, $\vec{q}_1=0$, $\vec{q}_2=0$, constant free surface and a cilindrical profile for the sediment layer:

$$h_2(x,y)=\begin{cases} 0.05 & \text{if } (x-0.5)^2+(y-0.5)^2\leq 0.01,\\ 0 & \text{otherwise.}\end{cases}$$

$$h_1(x,y)=0.1-h_2(x,y)-z_b(x,y).$$

The final time is set to $t=0.36$ s. and the frictional angle is $\delta_0=7^o$. In Figure 5 we can see the evolution of the sediment layer and the perturbation of the water surface. The water surface is pictured with colors in function of the module of the velocity. Red colors correspond to higger velocities. We can observe that the amplitude of the waves to the left and to the right of the rectangle are not exactly the same. Some differences on the velocity module can be also appreciated.

In Figure 6 we present a cut of the profiles at $y=0.5$. This figure has two columns. At the left colum we present the evolution of the free surface and the sediment layer. We can observe that the amplitude of the wave fronts are different. At the right column of Figure 6 we present a comparison of the velocities in the following form: we present the symmetric graph from $x=0.5$, in order to compare the velocity fronts. We can observe the influence of the bottom on the velocity. The velocity of the front is smaller to the right of the rectangle bump. And consequently the position of the wave front is delayed with respect to the position of the front to the left of the rectangle bump.

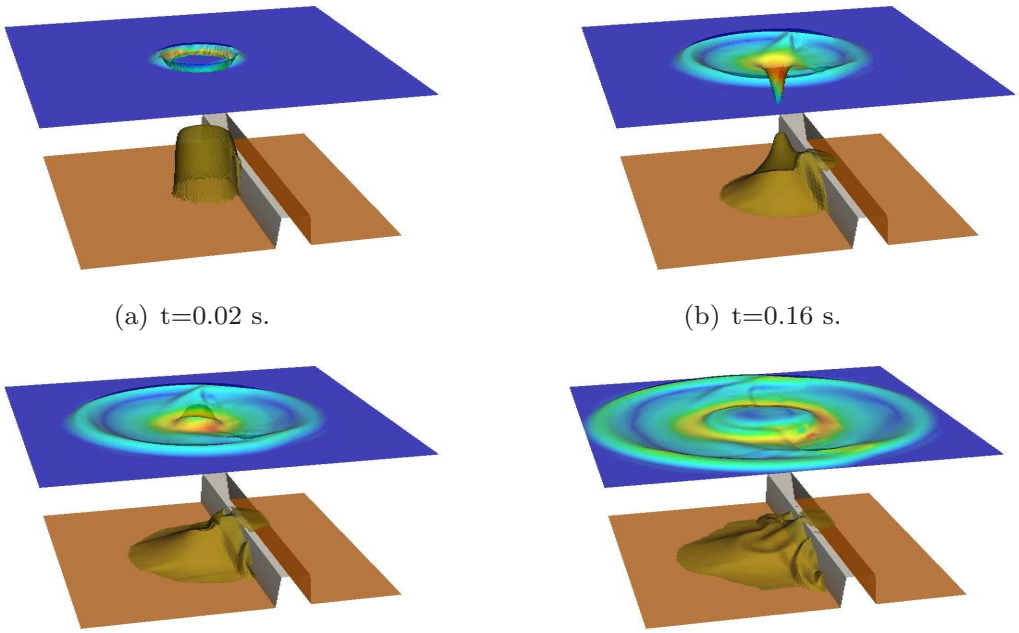

(a) t=0.02 s. (b) t=0.16 s.

(c) t=0.24 s. (d) t=0.36 s.

Figure 5: Submarine avalanche and generated tsunami

Acknowledgments

I would like to thanks all people who I have had the oportunity to collaborate with in different research papers. Specially to all the components of the research groups of Sevilla and Málaga directed by professors Chacón and Parés.

This research has been partially supported by the Spanish Government Research project MTM2006-01275 and P06-RNM-01594.

References

[1] M.J. Castro Díaz, T. Chacón Rebollo, E.D. Fernández-Nieto, J.M. González Vida. C. Parés. *Well-balanced finite volume schemes for 2D non-homogeneous hyperbolic systems. Application to the dam break of Aznalcóllar*. Comput. Methods Appl. Mech. Engrg. 197, no. 45-48, 3932-3950 (2008).

[2] M.J. Castro Díaz, E.D. Fernández Nieto, A.M. Ferreiro. *Sediment transport models in Shallow Water equations and numerical approach by high order finite volume methods*. Computers and Fluids, 37(3): 299-316, (2008).

[3] M.J. Castro, E.D. Fernández-Nieto, A. Ferreiro, J.A. García-Rodríguez, C. Parés. *High order extensions of Roe schemes for two-dimensional nonconservative hyperbolic systems*. J. Sci. Comput. 39, no. 1, 67-114 (2009).

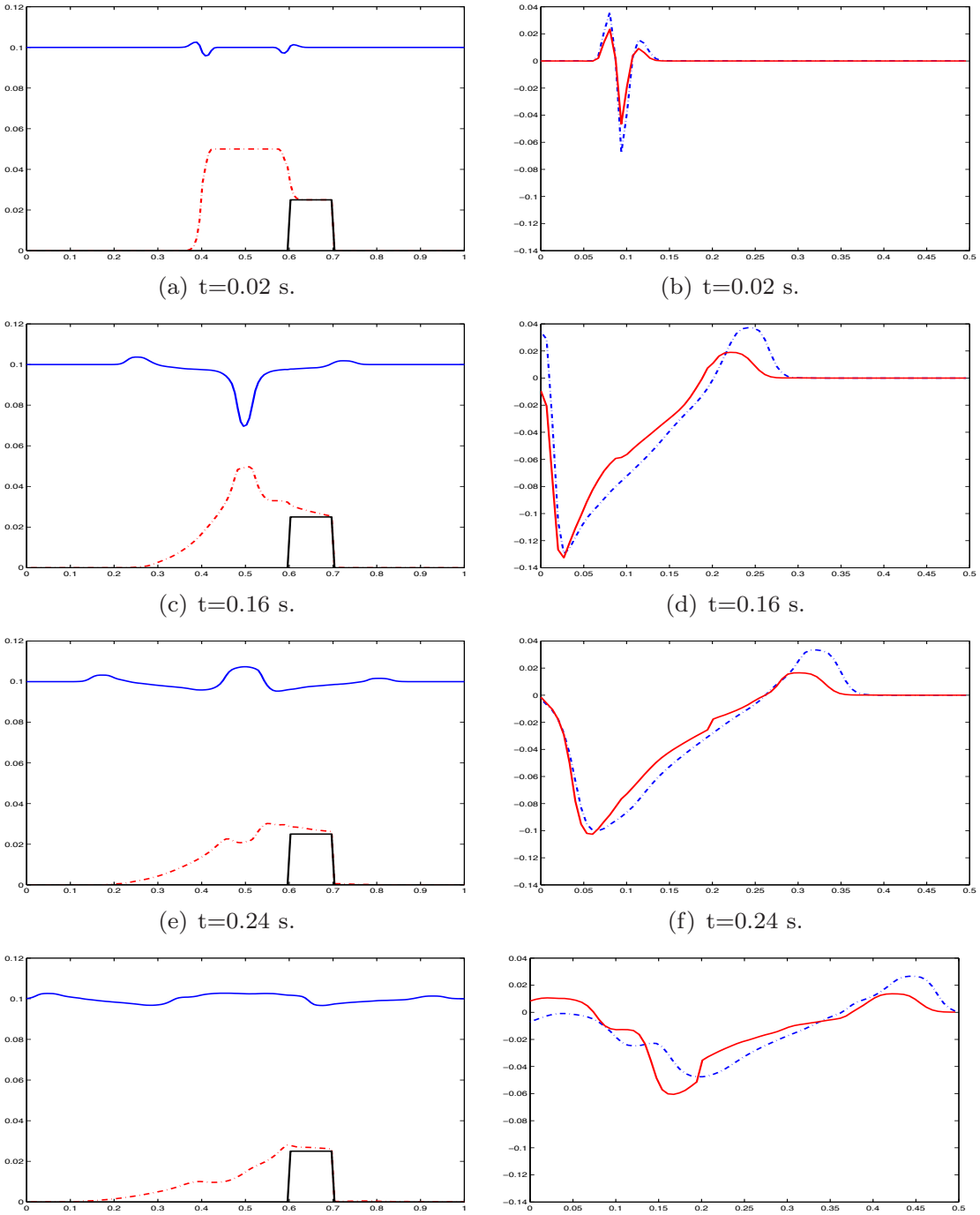

(a) t=0.02 s. (b) t=0.02 s.

(c) t=0.16 s. (d) t=0.16 s.

(e) t=0.24 s. (f) t=0.24 s.

(g) t=0.36 s. (h) t=0.36 s.

Figure 6: Left: Cut over the central edge of the domain (Water surface: continuous blue line. Sediment interface: dashed red line. Bottom: continuous black line). Right: Velocity comparison for the cut, from the center of the domain (Front to the right: continuous red line. Front to the left: dashed blue line)

[4] T. Chacón Rebollo, A. Domínguez, E.D. Fernández-Nieto. *A family of stable numerical solvers for the shallow water equations with source terms*. Comput. Methods Appl. Mech. Engrg. 192, no. 1-2, 203-225 (2003).

[5] G. Dal Maso, P.G. LeFloch, F. Murat. *Definition and weak stability of nonconservative products*. J. Math. Pures Appl. 74:483-548, (1995).

[6] H.J. De Vriend. 2DH Mathematical Modelling of Morphological Evolutions in Shallow Water. Coastal Engineering, vol, 11 1-27 (1987).

[7] H.J. De Vriend. *Analysis of Horizontally Two-Dimensional Morphological Evolutions in Shallow Water*. J. Geophys. Res. vol. 92, C4 3877-3893 (1987).

[8] H.A. Einstein *Formulas for the transportation of bed load*. Trans. ASCE. 107: 561-575, (1942).

[9] E. D. Fernández-Nieto, F. Bouchut, D. Bresch, M.J. Castro, A. Mangeney. *A new Savage-Hutter type model for submarine avalanches and generated tsunami*. J. Comput. Phys., 227(16): 7720-7754, (2008).

[10] E.D. Fernández-Nieto, D. Bresch, J. Monnier. *A consistent intermediate wave speed for a well-balanced HLLC solver*. C. R. Math. Acad. Sci. Paris 346, no. 13-14, 795-800 (2008).

[11] A. Ferreiro Ferreiro. *Desarrollo de técnicas de post-proceso de flujos hidrodinámicos, modelización de problemas de transporte de sedimentos y aproximación numérica mediante técnicas de volúmenes finitos*. Tesis Doctoral. Universidad de Sevilla (2006).

[12] E. Godlewski E, P.A. Raviart. *Numerical approximation of hyperbolic systems of conservation laws*. New York: Springer-Verlag, (1996).

[13] A.J. Grass. *Sediments transport by waves and currents*. SERC London Cent. Mar. Technol., Report No. FL29, (1981).

[14] J. Hudson.*Numerical technics for morphodynamic modelling*. Tesis doctoral. University of Whiteknights (2001).

[15] P.Y. Julien. *Erosion and Sedimentation*. Cambridge (1994).

[16] A.A. Kalinske *Criteria for determining sand transport by surface creep and saltation*. Trans. AGU. 23(2): 639–643, (1942).

[17] E. Meyer-Peter, R. Müller. *Formulas for bed-load transport*. Rep. 2nd Meet. Int. Assoc. Hydraul. Struct. Res., Stockholm: 39-64, (1948).

[18] T. Morales, M.J. Castro, C. Parés, E.D. Fernández-Nieto. *On a shallow water model for the simulation of turbidity currents*. Communications in computational physics, 848-882, vol. 6, (2009).

[19] A. Mangeney-Castelnau, J.P. Vilotte, M.O. Bristeau, B. Perthame, F. Bouchut, C. Simeoni, S. Yernini. *Numerical modeling of avalanches based on Saint-Venant equations using a kinetic scheme*. J. Geophys. Res.108 (B11), 2527 (2003).

[20] S. McDougall, O. Hungr, O. *Dynamic modelling of entrainment in rapid landslides*. Can. Geotech. J. 42, 1437-1448 (2005).

[21] P. Nielsen. *Coastal Bottom Boundary Layers and Sediment Transport*. World Scientific Publishing, Singapore, Advanced Series on Ocean Engineering, 4, (1992).

[22] C. Parés, M.J. Castro. *On the well-balance property of Roe's method for nonconservative hyperbolic systems. Applications to shallow-water systems*. ESAIM: M2AN, 38(5):821–852 (2004).

[23] C. Parés, M.L. Muñoz-Ruiz. *On some difficulties of the numerical approximation of nonconservative hyperbolic systems*. Bol. Soc. Esp. Mat. Apl. (SEMA), 47: 23-52 (2009).

[24] E. Peña González. *Estudio numérico y experimental del transporte de sedimentos en cauces aluviales.* Tesis Doctoral. Universidade da Coruña, (2002).

[25] M. Pirulli, A. Mangeney. *Result of Back-Analysis of the Propagation of Rock Avalanches as a Function of the Assumed Rheology.* Rock Mech. Rock Engng., 41(1), 59-84, (2008).

[26] O. Pouliquen, *Scaling laws in granular flows down rough inclined planes.* Phys. Fluid. 11, 542-548 (1999).

[27] M. Quecedo, M. Pastro, M.I. Herreros, J.a. Fernández Merodo, Qinfen Zhang, *Comparison of two mathematical models for solving the dam break problem using the FEM method*. Comput. Methods Appl. Mech. Engrg. 194, 3984-4005 (2005).

[28] S.B. Savage, K. Hutter, *The dynamics of avalanches of granular materials from initiation to run-out*, Acta Mech. 86, 201-223 (1991).

[29] E.F. Toro. *Shock-Capturing Methods for Free-Surface Shallow Flows.* Wiley and Sons Ltd. (2001).

[30] L.C. Van Rijn. *Sediment transport (I): bed load transport.* J. Hydraul. Div., Proc. ASCE, 110: 1431-56, (1984).

[31] J.D. Zabsonré, C. Lucas, E.D. Fernández-Nieto. *An energetically consistent viscous sedimentation model*. Math. Models Methods Appl. Sci. 19, no. 3, 477-499 (2009).

Enrique es licenciado en Ciencias Matemáticas en 1999 por la Universidad de Sevilla. También es doctor en Matemáticas en 2003 por la Universidad de Sevilla, recibiendo el Premio del Ayuntamiento de la ciudad hispalense a la mejor tesis doctoral en el área científco técnica. Actualmente es profesor Titular en el Departamento de Matemática Aplicada I de la Universidad de Sevilla.

En sus inicios la investigación se ha centrado en el estudio de esquemas de volúmenes finitos bien equilibrados para sistemas hiperbólicos no homogéneos y sus aplicaciones. Posteriormente, se ha dedicado al estudio de modelos y simulación numérica de flujos someros para problemas de erosión en avalanchas, avalanchas submarinas, transporte de sedimento y avalanchas de materiales rígido-viscoplásticos, entre otros.

Ha realizado varias estancias de investigación en la Universidad de Savoie, Instituto de Física Globe y Escuela Normal Superior de París, en Francia. Cabe destacar un gran número de colaboraciones con investigadores de varias universidades francesas, Universidad de Sevilla y Universidad de Málaga.

También ha codirigido dos tesis doctorales, con el profesor M.J. Castro de la Universidad de Málaga y el profesor D. Bresch de la Universidad de Savoie, respectivamente.